CGU HS Committee on River Ice Processes and the Environment
13th Workshop on the Hydraulics of Ice Covered Rivers
Hanover, NH, September 15-16, 2005

Field Measurements and Analysis of Waves Generated by Ice-Jam Releases

Spyros Beltaos

National Water Research Institute, Environment Canada,
867 Lakeshore Road, Burlington, ON, L7R 4A6, Canada
spyros.beltaos@ec.gc.ca

Upon the release of an ice jam, water and ice held by the jam are suddenly free to move. The resulting wave generates increased water stages and higher flow velocities, posing a risk to downstream structures, people, and aquatic life. Climate-induced changes to river ice processes, such as enhanced midwinter jamming or increased spring flows, could result in more frequent occurrence of major and damaging waves. Recently obtained field data sets on ice-jam generated waves are discussed and compared to existing theories. Wave celerity decreases along the waveform, being largest at the leading edge, intermediate at the crest, and least at the trailing edge. Celerity also tends to decrease with time and distance traveled. Very near the point of release, the leading-edge celerity approximates that of a gravity wave, dropping to near kinematic-wave values as travel distance increases. The presence of moving ice rubble prevents measurement of important hydrodynamic characteristics of a wave, such as flow velocity, discharge, and boundary shear stress. These quantities can be calculated, however, using an analytical method that is based on the equations of motion and on plausible approximations for natural-stream geometry. Application to a few case studies elucidates the degree to which a jam-release wave can magnify hydrodynamic forces. The steepest waves, which are observed closest to the point of release, generate the largest magnification, approaching an order of magnitude in one instance.

1. Introduction

An "ice-jam-release wave" is the dynamic discharge of water and ice from storage when an ice jam suddenly releases. As the wave travels downstream, it raises water levels and amplifies flow velocities, shear stresses, sediment transport rates, and rates of scour and erosion. High stages and ice runs created by the release of an upstream ice jam can carry away or damage bridge decks. The attendant high velocities can scour riverbeds, undermine bridge piers, erode stream banks, and degrade aquatic habitat; they can also contribute to damage of structures and property along the river, and can have major ecological impacts. The issue of climate change further underscores the need for improved knowledge of dynamic release phenomena because river ice processes are very sensitive to climatic conditions (Beltaos 1997; Beltaos and Prowse 2001). Until recently, release waves have been largely known from anecdotal reports and descriptions, owing to the many practical difficulties associated with field data collection.

In the past few years, detailed data sets have been obtained under field programs conducted in Yukon, Alberta and New Brunswick (Jasek 2003a, 2003b; Hicks 2003; Kowalczyk and Hicks 2003; Andres et al. 2003; Beltaos and Burrell 2005a, 2005b), which provide useful insights on the release-wave propagation process. The purpose of this paper is to present an overview of recent work and summarize the main quantitative findings. Following a discussion of background information and of instrumentation, typical data are presented and general wave propagation patterns identified. A new method of analysis is outlined next, and illustrated with a few case studies. This approach enables determination of important, but difficult to measure, wave properties, such as velocity, discharge, water surface slope and shear stress. Wave-induced amplification of these quantities is shown to vary with distance traveled, being most intense near the point of release.

2. Background Information

Few observations of waves released by ice jams have been reported, and most are qualitative or based on visual estimates. Mercer and Cooper (1977) observed a jam release on the Mackenzie River near Point Separation in 1973, which resulted in an estimated peak velocity of over 7.6 m/s after 30 minutes. Gerard et al. (1984) observed a moving pack of ice some 140 km long, which they attributed to a wave on the Yukon River that broke up the ice cover downstream, over a distance of 300 km in 16 hours (rate of advance = 5.2 m/s). Parkinson and Holder (1988) discussed observations made during the 1982 ice breakup on the Mackenzie River and showed that the flows resulting from ice-jam release far exceed published daily-average values at hydrometric stations. Beltaos et al. (1994) and Beltaos et al. (1998) described ice-jam releases at two sites on the Saint John River, respectively located in New Brunswick and Maine, USA. Peak surface velocities of about 3 m/s were deduced in both cases, based on visual estimates and timed movement of ice floes, and lasting for more than an hour. Based on aerial and ground-based observations in Northern Canada, Jasek (2003a, 2003b) provided excellent descriptions of, and important insights on, ice runs and ice breaking fronts that result from ice-jam releases. Typical wave configuration and concomitant ice conditions are illustrated in Fig. 1, which is reproduced from Jasek (2003b). Initially, the ice cover is intact and rises with the incoming wave. If the rise is sustained, the ice cover is dislodged, and a flux of ice sheets is observed until

the rubble from the jam arrives at the measurement site. The five-metre wave height that occurred in the case of Fig. 1 is rather large, but so is the duration of the rising limb of the wave, resulting in an average rate of rise of 0.00035 m/s (0.021 m/min).

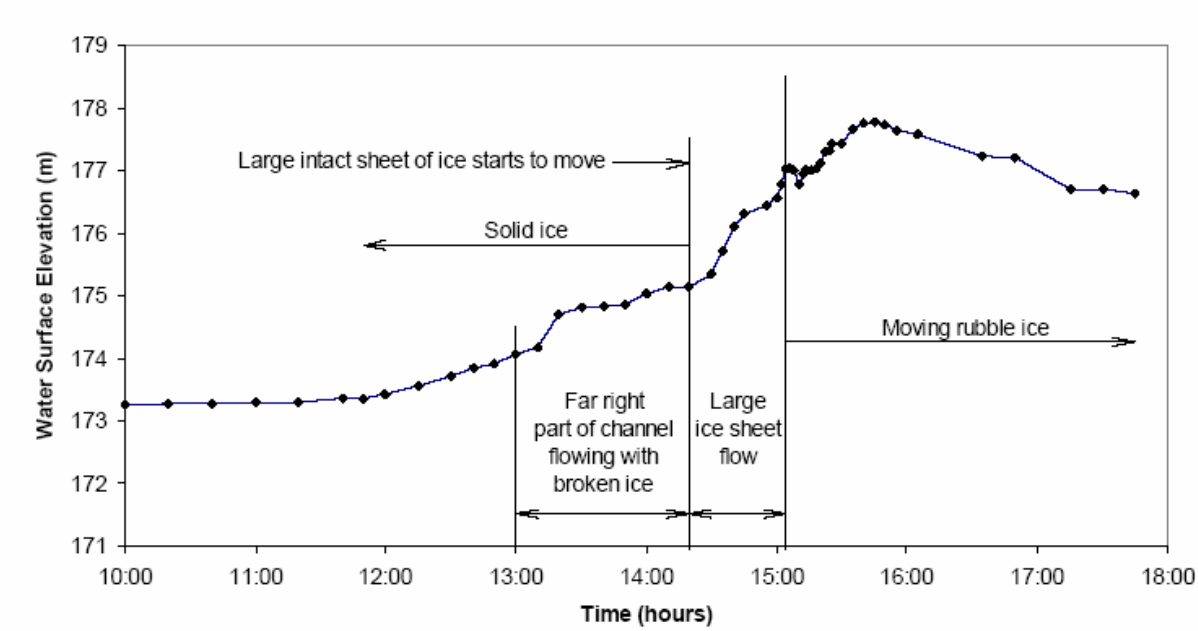

Figure 1. Water level and ice observations on the Hay River near Paradise Gardens, May 2, 1989. (from Gerard and Jasek 1990, as cited by Jasek, 2003b)

Hicks (2003) and Kowalczyk and Hicks (2003) reported detailed measurements of a large wave caused by the release of a 17 km long ice jam on the Athabasca River. This data set derives from continuous monitoring by pre-installed water-level gauges in a jam-prone reach, and is the most comprehensive that has been obtained to date. At the upstream-most gauge site, the water level rose 4.4 m in 15 minutes, which translates to an average rate of rise of 0.0049 m/s. This is an order of magnitude greater than the value associated with the wave of Fig. 1.

The earliest attempt to predict the characteristics of jam-release waves was made by Henderson and Gerard (1981), who developed an analytical solution, treating the release of an ice jam as a sudden removal of a vertical gate in an open channel. Other assumptions included a frictionless and horizontal bed, rectangular prismatic channel, infinite jam length, and an initial step-like profile. This idealization results in a step-like wave (or "surge") that comprises a lengthening reach of uniform flow between the upstream and downstream unperturbed-flow reaches. In the literature, the term "surge" has been applied extensively to waves that result from ice jam releases, regardless of how steep their rising limb might be. As will be shown later, real waves are far from being surges because their frontal slopes are miniscule relative to a step-like increase. For this reason the term surge is avoided herein, while the abbreviation JRW is used for convenience to denote a jam-release wave.

Attempts to predict JRW propagation and hydraulics in real rivers have focused on relatively simple conditions, where the effect of ice on the behaviour of the wave is most likely to be small (Beltaos and Krishnappan 1982). Consequently, waves have been simulated using one-dimensional hydrodynamic models developed for open-water conditions, with suitable flow-resistance adjustments where an ice cover is present (Mercer and Cooper 1977; Beltaos and Krishnappan 1982; Joliffe and Gerard 1982; Wong et al. 1985; Ferrick and Mulherin 1989; Saade et. al. 1993; Hicks et al. 1997; Blackburn and Hicks 2003; Andres et al. 2003). More recently, Liu and Shen (2004) applied a two-dimensional model to explore the effect of side friction on the motion of the rubble and thence, on wave propagation.

Though model output can be made to match measured wave forms with suitable choice of calibration parameters, reliable prediction of JRW propagation is still in the future. One limitation stems from the need to consider the effects of the ice cover, which may remain stationary, or be set in motion as a series of long sheets that eventually break down into rubble. A second limitation relates to logistics: while it is feasible to measure stage-time variation at specific locations, initial and boundary conditions are less amenable to measurement. Few JRW data sets include such ancillary information, and often involve a single waveform, so that model calibration cannot be checked at other locations along the river.

3. Field Instrumentation and Methodology

An obvious source of JRW data is the archived stage record of hydrometric gauging stations, such at those operated by Water Survey of Canada (WSC). Up to 1995, stage was recorded continuously on special charts, where steep waves are often discerned during the breakup period. A major obstacle to quantification of such data is the temporal chart resolution: unless a wave extends over several hours, it is not possible to accurately determine its shape. Starting in 1996, stage is recorded in digital format, providing readings at 15-minute, or greater, intervals. This approach does solve the chart resolution problem, but the recording interval may be too large (see also later discussion). Gauge-recorded waves on the same river are usually too far apart to allow detailed assessment of propagation characteristics, while there is no concurrent information on ice conditions or origin of the wave.

Obtaining comprehensive field data on JRWs can be daunting. The formation of an ice jam depends upon prevailing hydrologic and meteorological conditions, and these conditions may not occur during a single field season. Even if an ice jam forms, it may release suddenly and at a time, such as the middle of the night, when field measurements cannot be conveniently obtained. In addition, jams might occur along a river reach where accurate and detailed measurement of wave characteristics cannot be safely obtained. Accessibility to the river channel downstream of an ice jam and a capability for rapid deployment of water-level measurement devices are important factors in the success of field measurements.

Where there is a high probability of ice-jam formation at a known site, multiple waveforms can be measured by installing a series of pressure transducers or other water-level sensing devices, spaced at suitable distances downstream of the expected jam location. This setup was deployed

by Kowalczyk and Hicks (2003) on the Athabasca River above Fort McMurray, and resulted in a unique data set, partially reproduced in Fig. 2.

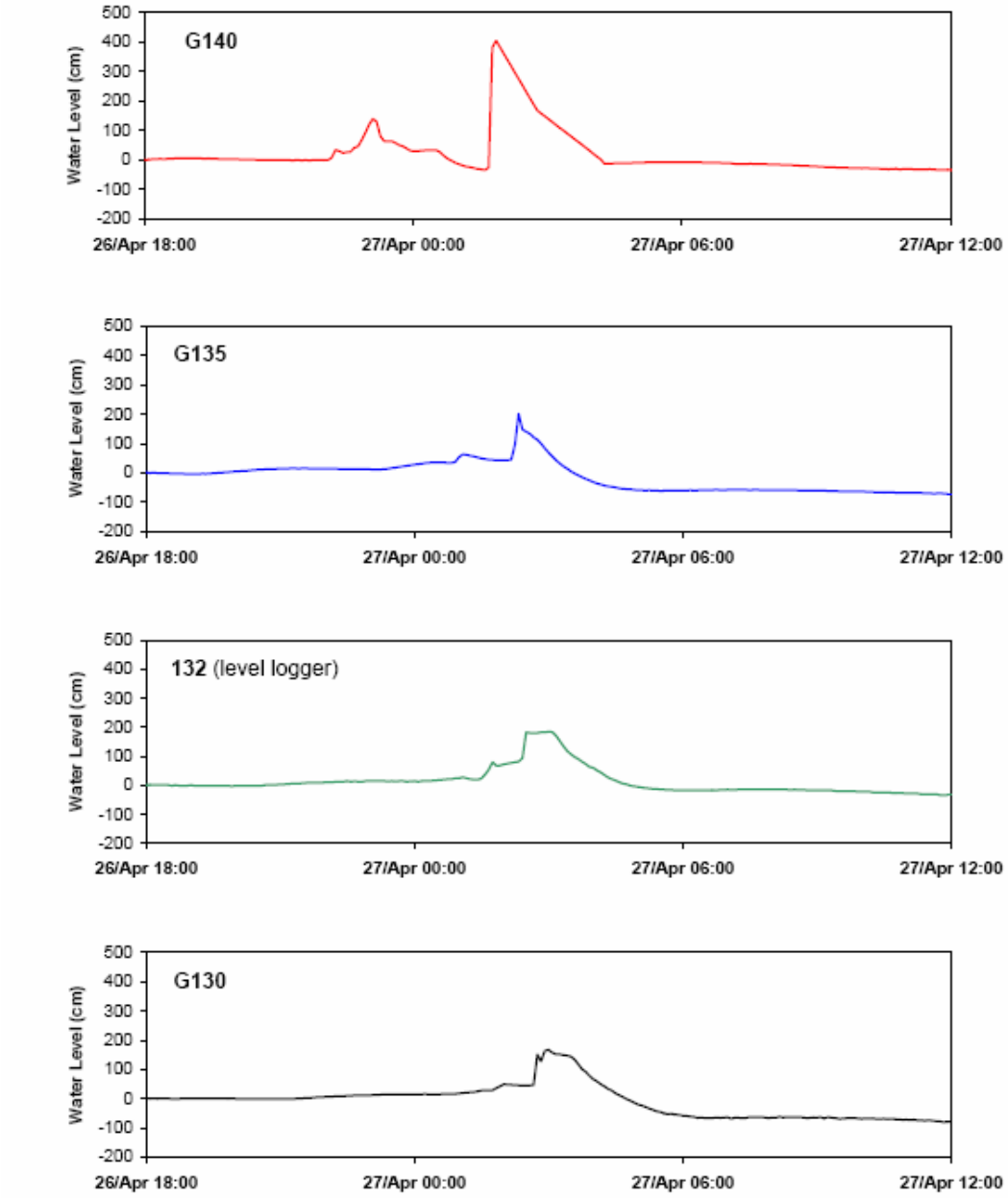

Figure 2. Waveforms obtained at consecutive monitoring stations on the Athabasca River above Fort McMurray, 2002. From Kowalczyk and Hicks (2003). Note progressive wave attenuation and dispersal.

For applications where the jam location and timing are unpredictable, a device called a "wave meter" has been developed at the National Water Research Institute of Environment Canada (Beltaos et al. 1998). The wave meter is portable and can be deployed easily and rapidly along

an accessible riverbank downstream of an ice jam. Once installed and activated, the meter remains stationary and reports, via radio-telemetry, the depth of water over it. The main advantage of the wave meter is that it can be deployed after a jam has formed. Of particular interest is the immediate vicinity of the jam toe (or downstream end), where the release wave is expected to be the most violent. Wave meters are often buried under grounded ice during the ice run that follows jam release but are retrievable after the ice rubble has melted. Several measurements of JRWs have been carried out in New Brunswick, using wave meters and pressure transducers, while the results are on occasion supplemented by hydrometric gauge records. These results have been reported by Beltaos and Burrell (2005a), and are briefly reviewed in the following sections.

4. Wave in Restigouche River, New Brunswick, April 2000

The lower Restigouche River forms the eastern boundary between New Brunswick and Quebec while the study reach extends from Camp Harmony to Flatlands (Fig. 3). An ice cover usually forms in November and breaks up in April. Breakup is typically triggered by runoff from snowmelt, often in combination with runoff from rainfall events. Due to the river's size (approx. 200 m wide) and slope (approx. 0.0008), major ice jams can form, causing severe release waves and ice runs, and resulting in considerable property damage and personal hardship (Beltaos and Burrell 2005a). Following a period of mild weather in late March, 2000, rising flows caused by rainfall and snowmelt, resulted in breakup of the ice cover of the Restigouche River. Broken ice jammed and released at several locations as it moved downstream.

Early in the morning of April 4, the toe of a jam was found at Mann Mountain Settlement. A wave meter was installed at 0700 h on the right bank of the river, 1 km below the mouth of Chessers Brook, or 1.5 km from the toe of the ice jam (Fig. 3). The jam was about 8 km long; at 0810 h, the head was located just below the mouth of the Upsalquitch River (Fig. 3). There was evidence of extensive grounding downstream of the toe, in the general vicinity of the mouth of Chessers Brook. Here, large ice slabs had been uplifted and were sagging between grounded pressure ridges. By 08:30 h, small pieces of ice were moving in a lead that had developed downstream of the toe. This occurred intermittently until the ice jam released at approximately 09:15 hours, generating the stage hydrograph shown in Fig. 4. The sheet ice cover below the jam was in motion at 09:17 h. For the next hour or so, the channel was full of running ice, with occasional openings. After that time, the surface concentration of ice began to decrease. Total water level rise during the passage of the wave was approximately 2.8 m, with the peak water level occurring some six minutes after the jam released. The average rate of rise was thus about 0.5 m/min. The river ran full of ice for about a half-hour, then the ice concentration gradually lessened. By 10:15 h, the surface concentration of ice was estimated to be about 80% but this had diminished to less than 20% by 10:30 h. Measurements were continued until about 10:55 hours.

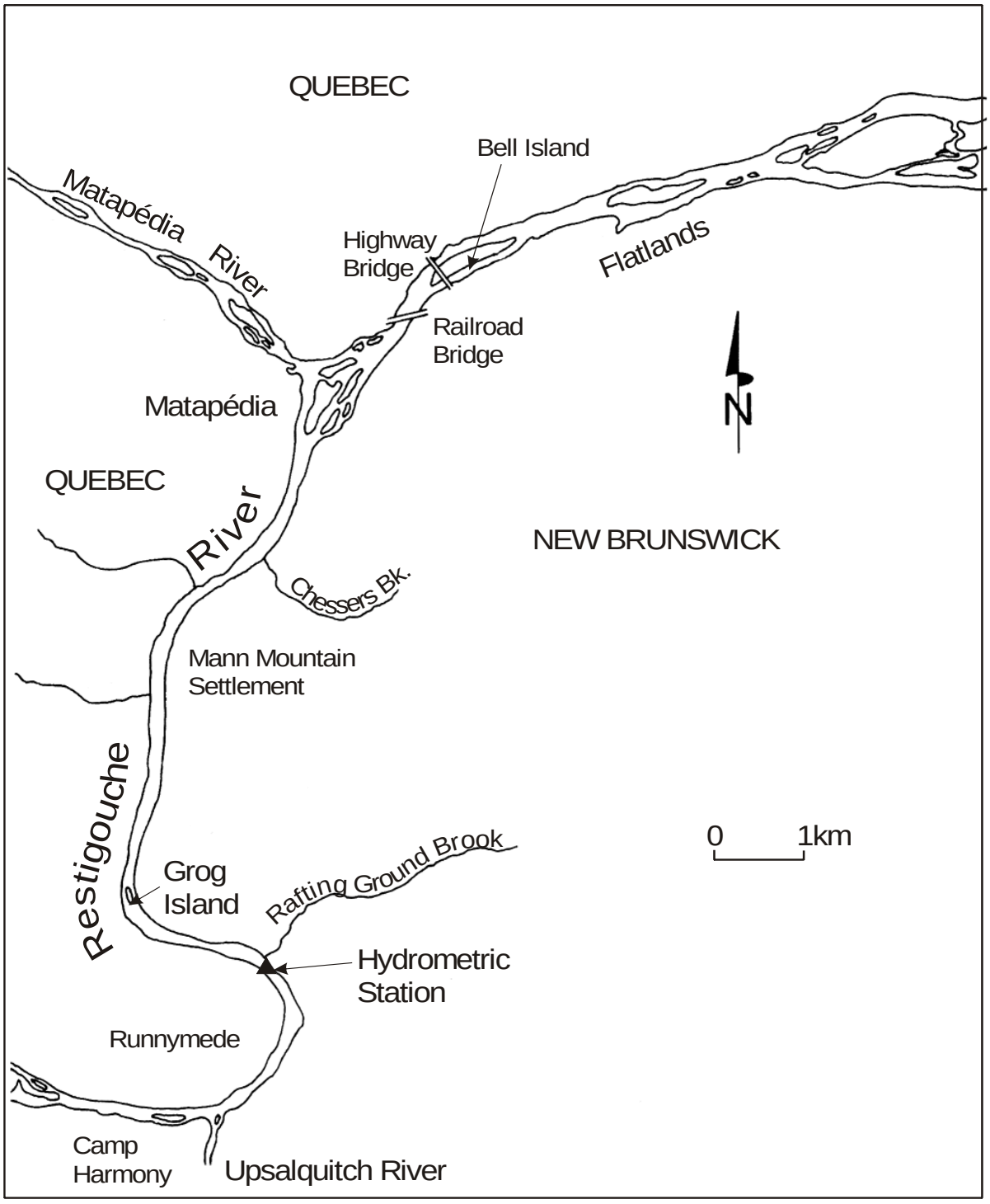

Figure 3. Restigouche River study reach

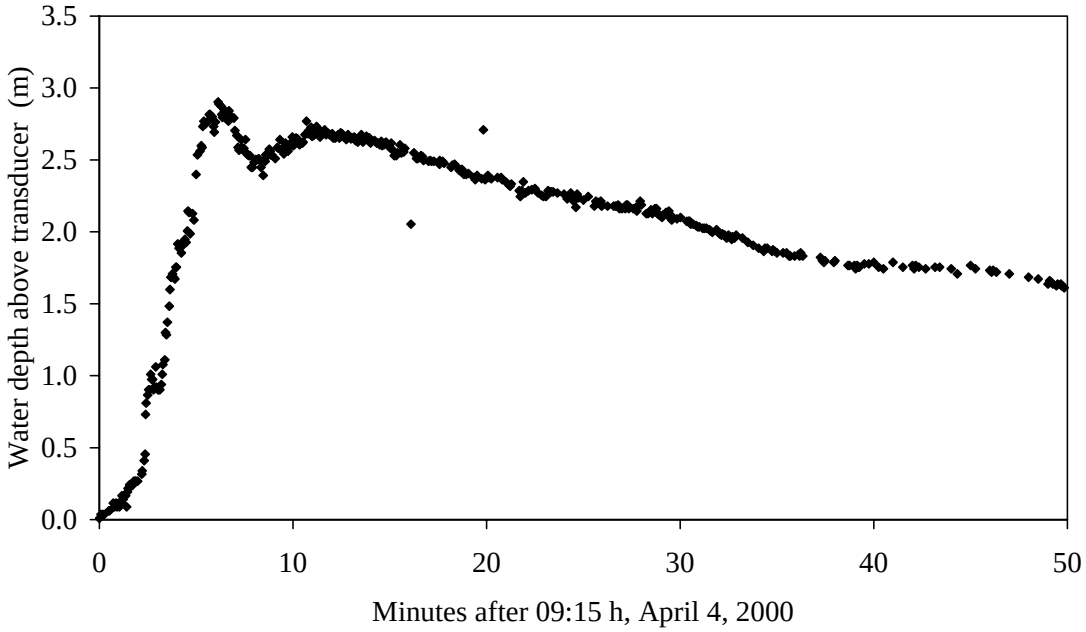

Figure 4. Stage recorded on the Restigouche River on April 4, 2000. From Beltaos and Burrell (2005a) with changes.

Fractured sheet ice was observed to be running by the community of Matapedia (~ 3.5 km downstream of the jam toe) and by the interprovincial railway bridge (4.1 km downstream of the toe) at 12 and 16 minutes after the release, respectively. Twenty minutes after release, fractured sheet ice was running at a site 6 km from the toe, about 1 km downstream of the inter-provincial highway bridge. These observations suggest that the leading edge of the wave was dislodging the sheet ice cover and moving at an average celerity of no less than 5 m/s during the first twenty minutes of its advance. Ice was still running past the two bridges some 90 minutes after the release, but it was now of the rubble variety, with a surface concentration of only 5% to 20% (varying across the river).

The highly dynamic nature of this waveform further suggests that the 15-minute recording interval of hydrometric gauging stations can be too coarse in cases where the release point happens to be located very close to the gauge. This is illustrated in Fig. 4: a random selection of stage values, taken at 15 minute intervals, would most probably have missed the peak stage and generated a much flatter waveform than the actual.

5. Wave in Saint John River, New Brunswick, April 2002

The study reach of the Saint John River extended from Ledges, Maine to Edmundston, New Brunswick (Fig. 5), for a total river distance of approximately 40 km. Water levels and flow data were available from hydrometric stations located at Fort Kent and Edmundston. Information from previous studies, including field observations and cross sections, was also available for the study reach.

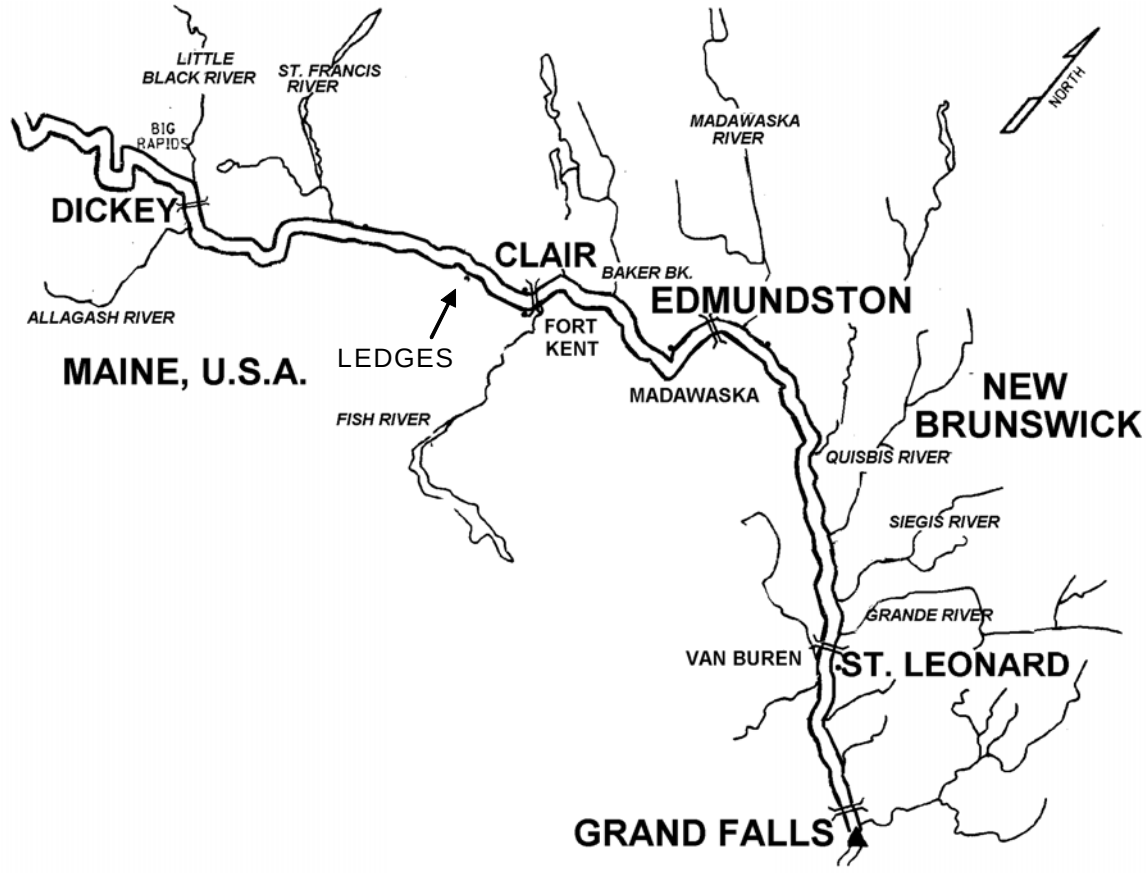

Figure 5. Upper Saint John River and wave study reach between Ledges and Edmundston. Channel width is exaggerated for illustration purposes.

On April 12, 2002, an ice jam formed in the Saint John River at Ledges. The toe of the ice jam was at km 104 and the wave meter was placed on the left (NB) bank at km 103.1, or 6.9 km upstream of the international bridge between Clair, NB and Fort Kent, Maine (Fig. 5). During the evening of the 12th, there were a few "runs" of rubble into open leads downstream of the toe, accompanied by brief spikes in the stage record. The jam released at about 1300 h, on April 13, generating a water-level rise of approximately 1.2 m in 70 minutes at Ledges. This wave, along with those recorded at downstream gauges are depicted in Fig. 6.

An initial inspection of the data revealed that characteristic features of the wave, such as the leading edge, the crest, and the trailing edge, do not propagate at the same rate. Respective average celerities were calculated from the available data for the reaches Ledges to Fort Kent gauge and Fort Kent gauge to Edmundston. These values are summarized in Table 1 and suggest that $C_L > C_P > C_T$ (in which C denotes celerity while the subscripts L, P, and T denote leading edge, peak stage, and trailing edge, respectively).

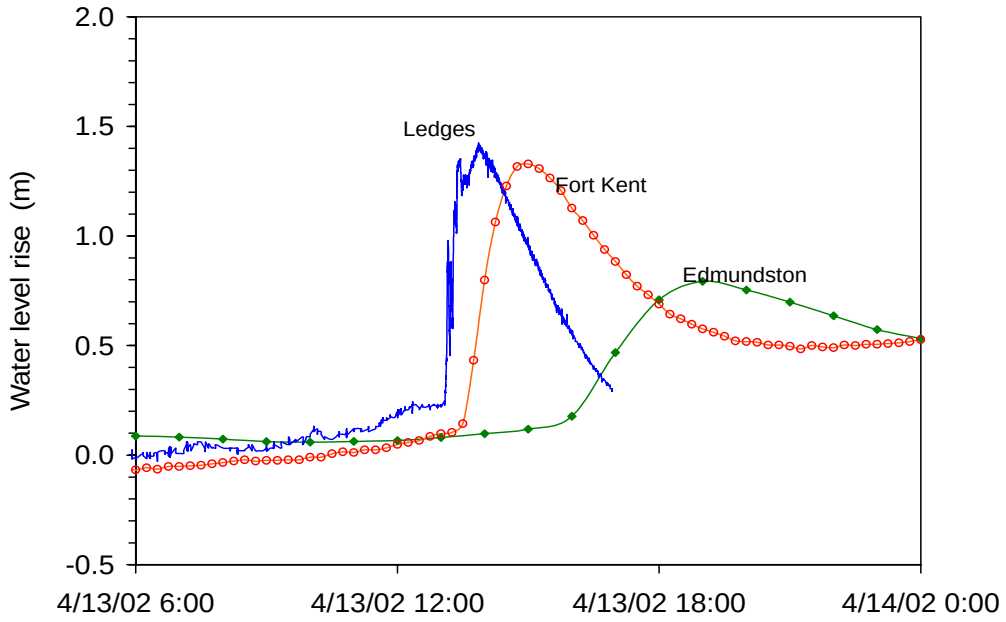

Figure 6. Saint John River surge of April 13, 2002, as registered at Ledges, Fort Kent, and Edmundston. Water level rise is above an arbitrary datum in each case. From Beltaos and Burrell (2005b) with changes.

Table 1. Estimated speeds of different wave features, Saint John River, April 13, 2002. From Beltaos and Burrell (2005a) with changes

Station	Distance between stations (km)	Maximum rise (m)	Average celerity between stations (m/s)		
			Leading edge	Peak stage	Trailing edge
Ledges		1.19			
	8.2		5.5	2.5	---(1)
Fort Kent gauge		1.19			
	32.2		3.5	2.1	1.7
Edmundston gauge		0.62			

(1) Difficult to identify the trailing edge

6. Comparison with the Athabasca River data set

As mentioned earlier, Hicks (2003) and Kowalczyk and Hicks (2003) presented data for a JRW that traveled down the Athabasca River near Fort Murray in April of 2002 (see also Fig. 2). From the information presented in these two references, the celerities associated with the wave can be calculated and are presented in Table 2. As with the Saint John River data, it can be seen from Table 2 that $C_L > C_P > C_T$ while both values generally decrease as the wave travels downstream. The crest celerity between stations G135 and G130 does not fit the decreasing trend, but this could be caused by errors in identifying the time of the peak, owing to the "flat" crest at station G130 (Fig. 2). The first measured wave (G140) is remarkable because it registered a very large rise (4.4 m) within a very short time interval (15 min). The resulting average rate of rise is 0.0049 m/s (0.29 m/min). By comparison, the Restigouche River wave caused a rise of 2.9 m in 6 minutes, resulting in an average rate of rise of 0.0081 m/s (0.48 m/min). Both waves were recorded very near the toe of the released jam (~ 1 to 1.5 km).

Table 2. Estimated celerities of ice jam release wave features, Athabasca River above Fort McMurray, April 27, 2002 (from Beltaos and Burrell 2005a with changes; based on data by Hicks 2003; Kowalczyk and Hicks 2003)

Station	Distance between stations (km)	Maximum rise (m)	Average celerity between stations (m/s)		
			Leading edge	Peak stage	Trailing edge
G140		4.4			
	5.4		4.3	3.2	2.3
G135		1.5			
	9.1		3.9	3.6	1.9
G130		1.2			
	10.7		3.3	2.5	--- (1)
G105		0.8			
	1.7		0.7	0.5	--- (1)
G95		1.0			

(1) Difficult to identify the trailing edge

7. Comparison with Theoretical Results

The small-amplitude wave theories (Ponce and Simons 1977; Daly 1993, 1995) suggest a common celerity for all points along the wave. This need not apply to a single wave of finite amplitude, and indeed the field measurements indicate that the celerity decreases along the wave form, being largest at the leading edge and least at the trailing edge. Therefore, the waveform spreads out and attenuates as it travels downriver.

The small-amplitude theory indicates further that, in general, the celerity should be between the kinematic value ($C_k = 1.5U_o$) and the gravity value ($C_g = \sqrt{g h_o} + U_o$). In natural streams, these quantities are typically about 1.5 m/s and 6 m/s, respectively. Inspection of Tables 1 and 2 indicates that the value of C_g is only approached by the leading-edge celerity, and especially near the toe of the released jam. Tables 1 and 2 also suggest that the celerity of the peak tends to be closer to the kinematic value, which is similar to the crest celerity of runoff-generated flood waves.

The theory of Henderson and Gerard (1981) neglects friction and bed-slope effects, and results in a true surge, that is, a step-like rise in stage. The celerity of this surge scales on $(gh_o)^{1/2}$ and exceeds that of a gravity wave by an amount that depends on the relative backwater caused by the jam prior to its release. The available field data indicate celerities that are generally less than C_g, though it is possible that higher values may briefly occur at the very toe of the jam. With reference to the step-like feature of a surge, it is noted that the fastest water-level rise that has been documented to date is about 0.5 m/min, which is a fearsome prospect for residents of nearby floodplains, or construction crews working on river structures. However, the corresponding frontal wave slope (calculated using a wave celerity of ~ 6 m/s) is of the order of 0.001. It is thus evident that a JRW, though dangerously steep, is not a surge - not even approximately. This result suggests that the conditions associated with surge formation (frictionless and horizontal river bed) may be too restrictive.

8. Rising-Limb Analysis

To assess hydrodynamic wave characteristics that are difficult to measure when ice is present, Beltaos and Burrell (2005b) proposed an analytical method that utilizes the one-dimensional equations of motion of river flow. By means of partial differentiation and integration, the following equation was obtained for the rising limb of the wave:

$$\frac{\partial y}{\partial t} \approx \frac{C(S_f - S_o)}{1 - a\frac{U^2}{gh} + \frac{C^2}{gh}\left(\frac{(1+a)U}{C} - 1\right)} \qquad [1]$$

in which, S_o = unperturbed-flow river slope; S_f = friction slope, calculated in terms of velocity and hydraulic radius using the Manning resistance equation; t = time; U = average flow velocity; C = celerity of the waveform; g = gravitational acceleration; y = water depth = water surface elevation minus bed invert elevation; h = average flow depth, empirically known to vary in proportion to y, such that h = ay, with a = site- or reach-specific dimensionless coefficient (a = 1 for rectangular channels, and less than 1 for natural bathymetries); and q_o = unperturbed-flow discharge per unit river width.

From the equation of continuity, the average flow velocity, U, can be expressed as:

$$U = \frac{q_o + \int_{y_o}^{y} C\,dy}{h} \qquad [2]$$

The integration on the right-hand-side (RHS) of Eq. 1 indicates that C is not a constant, but changes along the waveform, a property that is responsible for the looped appearance of the stage-flow variation during the passage of the wave.

In deriving Eq. 1, the frozen-wave approximation was invoked, under which the total derivative Dy/Dt is set equal to zero, so that $\partial y/\partial t + C\,\partial y/\partial x \approx 0$. This assumption is reasonable along the rising limb of the wave, where spatial and temporal derivatives are relatively large in absolute value. It is not reliable in the wave crest region or along the falling limb, where both derivatives are small in magnitude or even zero. However, the rising limb is the most dynamic portion of the wave, because it is here that velocity, flow, and shear stress are highest.

Using Eq. 1, together with Eq. 2, the value of $\partial y/\partial t$ can be computed as a function of y, given an assumed variation of C with y. This can be done by specifying the leading-edge celerity (C_L) and the value at the wave peak (C_P), in conjunction with an interpolation function. Consequently, $\partial y/\partial t$ can be determined from Eq. 1 as a function of y for a large number of incremental y-values that represent the range y_o to y_{peak}. For the N^{th} depth (or elevation) interval, Δy, a corresponding time increment is calculated as

$$\Delta t_N = \frac{\Delta y_N}{\frac{1}{2}\left[\left(\frac{\partial y}{\partial t}\right)_{N-1} + \left(\frac{\partial y}{\partial t}\right)_N\right]} \qquad [3]$$

By summing the time increments, a set of time values can be applied to any selected set of elevations or depths. The resulting relationship can be compared with the rising limb of the measured wave, and the input parameters (C_L, C_P) adjusted until agreement is optimized.

Alternatively, Eq. 1 can be integrated by means of a Runge-Kutta algorithm after inverting Eq. 1:

$$\frac{\partial t}{\partial y} = f(y) \approx \frac{1}{C(S_f - S_o)}\left[1 - a\frac{U^2}{gh} + \frac{C^2}{gh}\left(\frac{(1+a)U}{C} - 1\right)\right] \qquad [4]$$

Consequently,

$$t_{N+1} = t_N + \frac{\Delta y_N}{6}\left(k_1 + 2k_2 + 2k_3 + k_4\right) \qquad [5]$$

in which Δy_N = small increment in y between the times t_N and t_{N+1}; it may be fixed throughout the integration range, or it may vary in user-specified manner. The k-factors are defined by:

$$k_1 = f(y_N)$$
$$k_2 = f(y_N + \frac{\Delta y_N}{2}) \quad \textit{approximated as } [f(y_N) + f(y_{N+1})]/2$$
$$k_3 = f(y_N + \frac{\Delta y_N}{2}) = k_2 \qquad [6]$$
$$k_4 = f(y_N + \Delta y_N) = f(y_{N+1})$$

The Runge-Kutta technique is more robust than the more intuitive, finite-difference scheme used by Beltaos and Burrell (2005b) and requires fewer elevation and time increments.

The computational procedure can be conveniently programmed in a spreadsheet, where input parameters (C_L, C_P, and m) can be varied until the instantly calculated and plotted rising limb of the wave coincides with the measured one. Once the optimum values of the input parameters have been selected, it is possible to determine other important hydraulic parameters of the wave, such as instantaneous discharge, average flow velocity, and flow shear stress. These computations are performed automatically in appropriate columns of the spreadsheet.

Beltaos and Burrell (2005b) applied the rising-limb analysis method (RLAM) to their measured wave forms on the Restigouche and Saint John Rivers with good results. Examples are illustrated in Figures 7 and 8. In the case of the Restigouche River wave, which was recorded very near the point of release (~ 1.5 km), the celerities C_L and C_P are equal (6.7 m/s), resulting in constant celerity throughout the rising limb. This value is approximately equal to the local celerity of a gravity wave (6.6 m/s). For the Saint John River wave at Edmundston, which was recorded at a distance of ~ 41 km from the point of release, the selected values of C_L and C_P were 3.4 and 2.0 m/s, respectively. Both are less than the local gravity-wave celerity of 5.9 m/s, while C_p is slightly less than the local kinematic-wave value of 2.3 m/s.

The analysis also showed that the wave can greatly magnify flow velocity, discharge, and shear stress near the point of release. This was particularly apparent in the case of the Restigouche River wave, where the calculated maximum wave discharge amounted to ten times the pre-release value. At the same time, the bed shear stress increased six-fold. Amplification factors decrease as the wave attenuates with distance and time from release. For the Edmundston wave form, which was measured some 41 km below the point of release, the RLAM indicated discharge and shear stress amplifications of 1.6 and 1.3, respectively (Beltaos and Burrell 2005b). In all cases, the flow velocity was less than both C_L and C_P, suggesting that the wave travels ahead of the rubble from the released jam, in accordance with experience (e.g. Jasek 2003a, 2003b) and theory (Henderson and Gerard 1981).

An interesting corollary of Eq. 1 is that, under normal conditions, the leading-edge celerity of the wave should be less than or equal to C_g, the gravity-wave value (see Appendix A). This result is supported by the above findings, though in the case of the Restigouche River wave, C_L was slightly higher than C_g (6.7 m/s as opposed to 6.6 m/s).

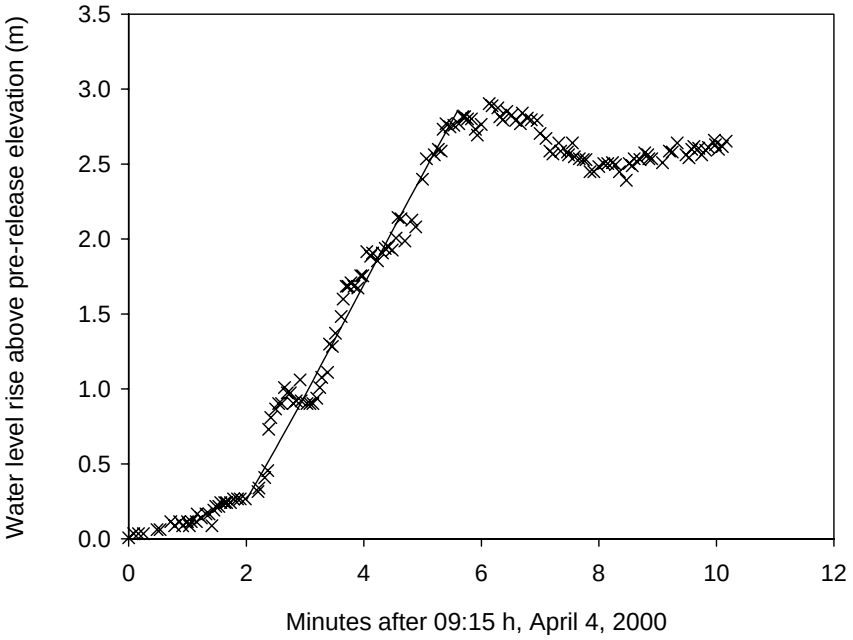

Figure 7. Comparison between calculated (line) and measured (data points) water levels during the rising portion of the Restigouche River wave at Walker's camp ($C_L = C_P = 6.7$ m/s). From Beltaos and Burrell (2005b) with changes

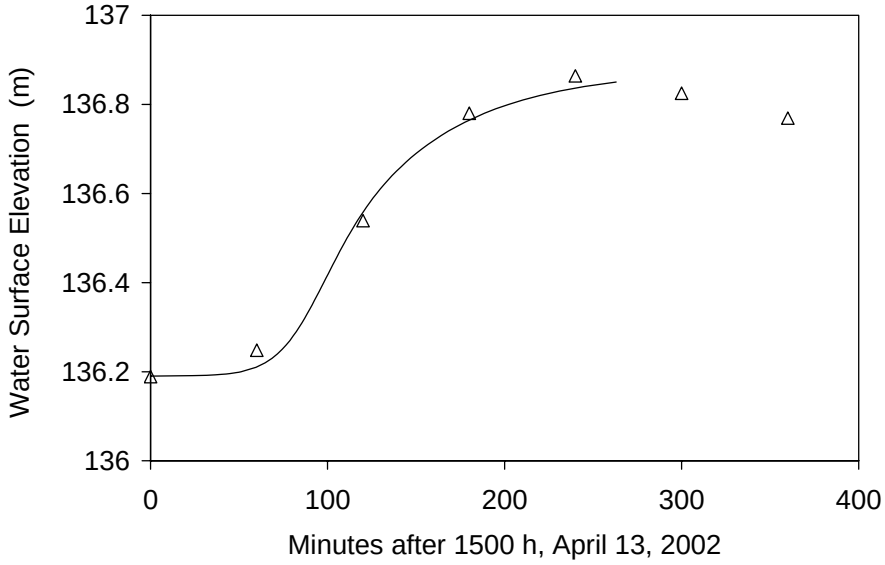

Figure 8. Comparison between calculated (line) and measured (data points) water levels during the rising portion of the Saint John River wave at Edmundston ($C_L = 3.4$ m/s; $C_P = 2.0$ m/s). From Beltaos and Burrell (2005b) with changes

9. Comparison of RLAM with numerical model output

It is not possible at present to directly corroborate the RLAM, because the presence of stationary and moving ice precludes deployment of suitable instruments, such as current meters, to measure velocity and discharge. However, the leading-edge and peak-stage celerities deduced by the RLAM were consistent with respective average values between sites where the waveforms were measured. More detailed tests can be performed by applying the RLAM to numerically-generated waves, for which not only point-values of celerity, but also flow velocity and discharge can be determined. This type of comparison was carried out by Beltaos and Andres (2005) who examined a wave generated by the collapse of a winter ice cover (Peace River, Alberta). In that study, rising-limb velocities and flows generated by a dynamic flow model (Hicks 1996) were in satisfactory agreement with corresponding values obtained from the RLAM.

As a further test of the RLAM, the model "River1d" (updated version of the Hicks model) was applied to a hypothetical jam-release wave in a rectangular prismatic channel, by assuming the initial conditions indicated in Fig. 9. The water surface profile approximates that which might be caused by a 7 km jam, forming in a 120 km long reach of open water. Boundary conditions consisted simply of: (a) flow = constant = 364 m^3/s at the upstream end of the modelled reach, or 0 km; and (b) water level = constant = 82. 5 m at the downstream end of the modelled reach, or 120 km.

Four model-generated waveforms at different locations downstream of the jam were matched using the RLAM, and a typical result is shown in Fig. 10. Corresponding flows are compared in Fig. 11 and shown to be close, though the analytical method over-predicts near the wave crest. As discussed earlier, this is probably due to the frozen-wave approximation breaking down in the vicinity of the crest. Nevertheless, the local discrepancy only amounts to 11%. The same type of comparison applies to flow velocity, which is directly proportional to discharge. In the case of shear stress, which is proportional to the square of velocity, the maximum discrepancy would amount to 22%.

By examining model-generated waveforms at successive stations, herein spaced at 1 km intervals, it is possible to determine approximate point-values of celerity for the leading edge and peak stage, and compare them with values indicated by the analytical method. The results of this operation are summarized in Table 2 and, with one exception, seen to be in good agreement. In all cases, C_L and C_P are between the applicable kinematic- and gravity-wave celerities, 6.41 and 2.18 m/s, respectively.

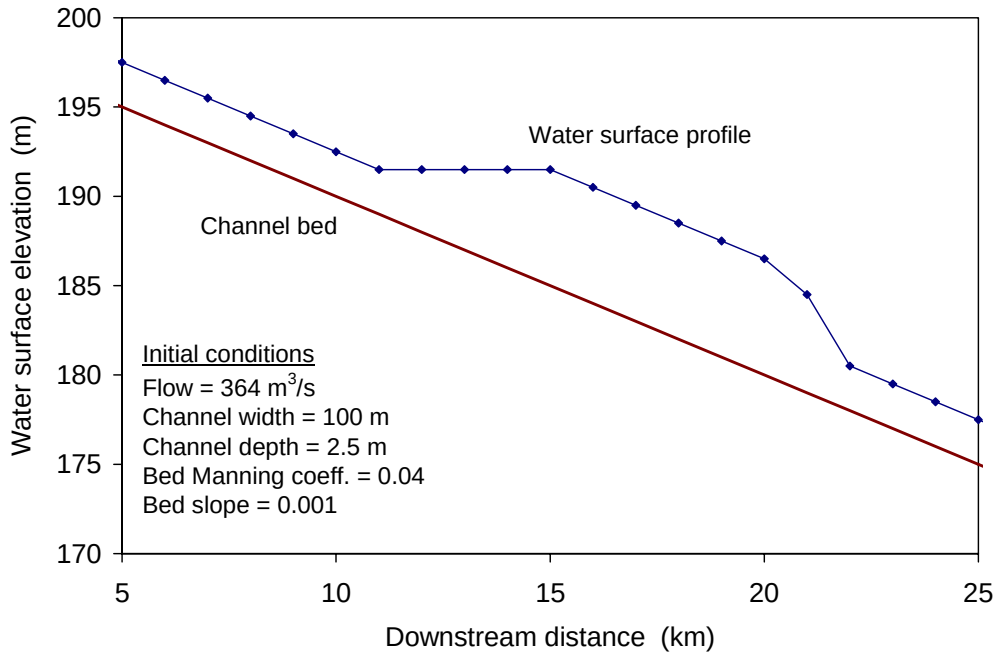

Fig. 9. Assumed initial conditions and water surface profile caused by an ice jam in an open-water reach of a hypothetical channel

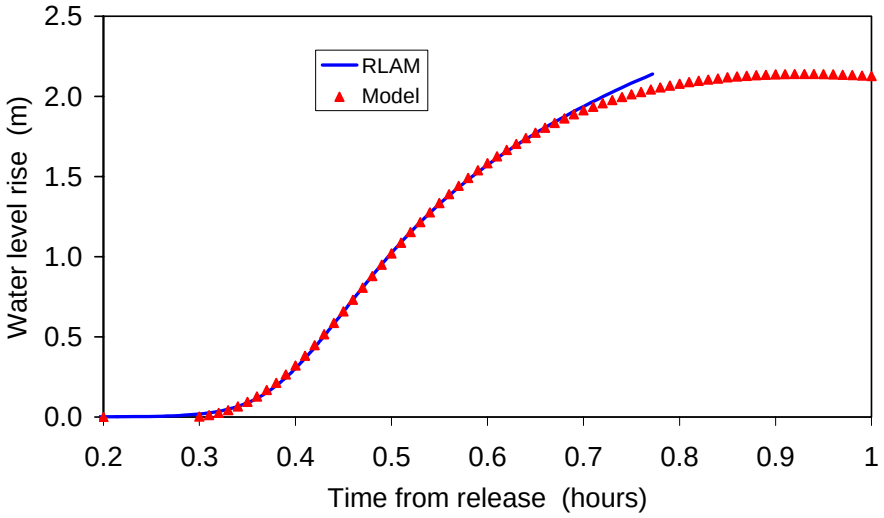

Fig. 10. Matching the rising limb of the model-generated waveform at a site located 7 km below the toe of the jam

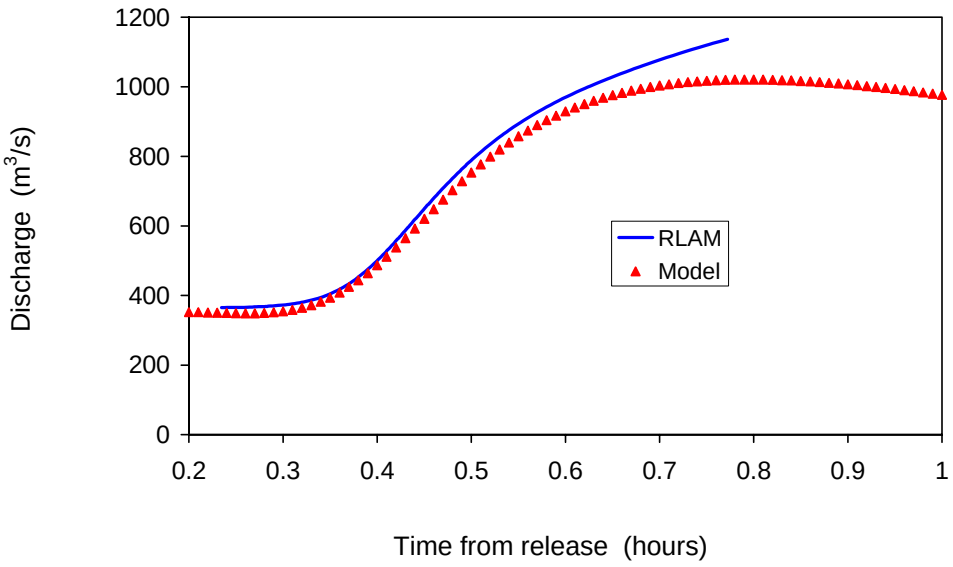

Fig. 11. Comparison between analytically-derived and model-generated flows at a site located 7 km below the toe of the jam

Table 2. Analytical versus model-generated celerities

Waveform location (km below toe of jam)	Wave height (m)	From RLAM		From numerical model output	
		C_L (m/s)	C_P (m/s)	C_L (m/s)	C_P (m/s)
1	2.77	6.05	3.90	6.17	2.94
7	2.13	4.63	2.92	4.63	2.92
17	1.72	4.00	2.64	3.97	2.65
47	1.18	3.27	2.60	3.09	2.65

10. Concluding Remarks

Water waves and ice runs generated by the release of ice jams can result in loss of human life, in damage or destruction of infrastructure, in devastation of private property, and in diverse impacts on the biophysical environment. An ability to predict the characteristics and effects of ice-jam release waves may lead to further development of strategies to reduce losses. Along many Canadian rivers, changing climates will likely result in changes in the frequency and severity of ice jams, and thus in the occurrence and nature of ice jam release waves.

Recent field studies have shown that the celerities of various components of the wave that is produced upon release of an ice jam differ, with the celerity of the leading edge being greater

than the celerity of the wave peak, while the latter is greater than the celerity of the trailing edge. Moreover, the data suggest that the wave slows down as it travels, so that the celerity of any one component of the wave decreases with distance from the point of release.

The measured waves differ from idealized waves deriving from simplifying theoretical hypotheses, such as small amplitude and linearization of the equations of motion, or neglect of hydraulic resistance and channel slope. It is only very near the point of release, i.e. during the very early phase of the wave propagation, that the wave celerity approaches that of the gravity-type of wave, which is the maximum celerity indicated by the small-amplitude theory. In this early phase, the rising limb of the wave is very steep but still far from the step-like increase predicted by the zero-resistance/slope theory.

To compensate for experimental difficulties associated with insitu measurement of flow velocity and shear stress, the equations of motion can be used in conjunction with measured waveforms to calculate such quantities along the rising limb of the wave. The resulting analytical method has been successfully applied to a few field measurements, and provides useful insights on the amplification of hydrodynamic wave characteristics as a function of time and distance traveled. While direct corroboration of this approach is not possible at present, application to waveforms generated by numerical models indicates agreement between analytical and model-generated celerities and velocities.

Acknowledgment

The author is indebted to Professor Faye Hicks, University of Alberta, who kindly made available the model River1d and provided helpful advice on how to run it.

References

Andres, D., Van Der Vinne, G., Johnson, B., and Fonstad, G. 2003. Ice consolidation on the Peace River: release patterns and downstream surge characteristics. Proceedings (CD format), 12th Workshop on the Hydraulics of Ice Covered Rivers, CGU HS Committee on River Ice Processes and the Environment, Edmonton, AB, June 19-20, pp. 319-330.

Beltaos, S. 1997. Effects of Climate on River Ice Jams. Proceedings, 9th Workshop on River Ice, Fredericton, Canada, pp. 225-244.

Beltaos, S., and Andres, D.D. 2005. Hydrodynamic characteristics of waves released by ice cover consolidation: Peace River below Dunvegan. Proceedings CD, 13th Workshop on the Hydraulics of Ice Covered Rivers, Hanover, NH, USA.

Beltaos, S. and Burrell, B.C. 2005a. Field measurements of ice-jam-release surges. Canadian Journal of Civil Engineering, in press.

Beltaos, S. and Burrell, B.C. 2005b. Determining ice-jam surge characteristics from measured wave forms. Canadian Journal of Civil Engineering, in press.

Beltaos, S., and Krishnappan, B.G. 1982. Surges from ice jam releases: a case study. Canadian Journal of Civil Engineering, 9(2): 91-110.

Beltaos, S., and Prowse, T. D. 2001. Climate impacts on extreme ice jam events in Canadian rivers, Hydrological Sciences Journal, 46(1): 157-182.

Beltaos, S. and Rowsell, R. 2001. Field Study of Pre-Breakup River Waves. Proceedings (available in CD format), 11th Workshop on River Ice, Ottawa, Canada, 4-17.

Beltaos, S., Burrell, B.C., and Ismail, S. 1994. Ice and sedimentation processes in the Saint John River, Canada. Proceedings International Ice Symposium, of IAHR, Trondheim, Norway, August 1994, Vol. 1, pp. 11-21.

Beltaos, S., Ford, J.S., Burrell, B.C., Pedrosa, M., and Madsen, N.K. 1998. Remote measurements of temperature and surge levels in ice-laden rivers. Proc., 14th International Ice Symposium, July 1998, Potsdam, NY, USA, Vol. 1, pp. 35-40.

Blackburn, J., and Hicks, F. 2003. Suitability of dynamic modelling for flood forecasting during ice jam release surges. Journal of Cold Regions Engineering, American Society of Civil Engineers, 17(1): 18-36.

Daly, S.F. 1993. Wave propagation in ice-covered channels. Journal of Hydraulic Engineering, ASCE, 119(8): 895-910.

Daly, S.F. 1995. Fracture of river ice covers by river waves. Journal of Cold Regions Engineering, ASCE, 9(1): 41-52.

Ferrick, M.G. and Goodman, N.J. 1998. Analysis of linear and monoclinal river wave solutions. US Army CRREL Report 98-1, Hanover, NH. USA, 24 p.

Ferrick, M.G., and N. D. Mulherin, 1989. Framework for control of dynamic ice breakup by river regulation. Journal of Regulated Rivers: Research & Management, 3, pp. 79-92.

Gerard, R., and Jasek, M. 1990. Break-up observations and ice jam flood forecast algorithm evaluation, Hay River, NWT, 1989. Report prepared for Indian and Northern Affairs Canada, Yellowknife, NWT. Department of Civil Engineering, University of Alberta, Water Resources Engineering Report 90-3, Edmonton, AB.

Gerard, R., Kent, T.D., Janowicz, R., and Lyons, R.O. 1984. Ice regime reconnaissance, Yukon River, Yukon. Proceedings of the 3rd International Specialty Conference on Cold Regions Engineering, 4–6 April 1984, Edmonton, Alta. Compiled and edited by D.W. Smith. Canadian Society for Civil Engineering, Montréal, Quebec, pp. 1059–1073.

Henderson, F.M., and Gerard, R. 1981. Flood waves caused by ice jam formation and failure, Proceedings IAHR Symposium on Ice, Quebec, Canada, Vol. I, pp. 277-287.

Hicks, F.E. 1996. Hydraulic flood routing with minimal channel data: Peace River, Canada. Canadian Journal of Civil Engineering. Vol. 23, No. 2 pp. 524-535.

Hicks, F.E. 2003. Modelling the interaction of climate, hydrology and river ice hydraulics, Mackenzie GEWEX Study (MAGS) Phase 2, Proceedings, 8th Scientific Workshop, Jasper, AB, Nov. 6 -8, 2002, edited by Peter di Cenzo, Saskatoon, Canada, pp. 151-161.

Hicks, F., McKay, K., and Shabayek. 1997. Modeling an ice jam release surge on the Saint John River, New Brunswick. Proceedings of the 1997 Workshop on River Ice, Committee on River Ice Processes and the Environment, Hydrology Section, Canadian Geophysical Union, Sidney, British Columbia, pp. 174-184.

Jasek, M. 2003a. Ice jam release surges, ice runs and breaking fronts – field measurements, physical descriptions and research needs. Canadian Journal of Civil Engineering. 30: 113-127.

Jasek, M. 2003b. Ice jam release and break-up front propagation. Proceedings (CD format), 12th Workshop on the Hydraulics of Ice Covered Rivers, CGU HS Committee on River Ice Processes and the Environment, Edmonton, AB, June 19-20, pp. 348-368.

Joliffe, I., and Gerard, R. 1982. Surges released by ice jams. Proceedings of the Workshop on Hydraulics of Ice-Covered Rivers, June 1 and 2, 1982, Edmonton, Alberta. Compiled by D.D. Andres and R. Gerard. Subcommittee on Hydraulics of Ice-Covered Rivers, Associate Committee on Hydrology, National Research Council of Canada, Ottawa, Ontario, Canada, pp. 253-259.

Kowalczyk, T. and Hicks, F. 2003. Observations of Dynamic Ice Jam Release on the Athabasca River at Fort McMurray, AB. Proceedings (CD format), 12th Workshop on the Hydraulics of Ice Covered Rivers, CGU HS Committee on River Ice Processes and the Environment, Edmonton, AB, June 19-20, pp. 369-392.

Liu, L., and Shen. H.T. (2004) Dynamics of ice jam release surges. Proceedings of the 17th International Symposium on Ice, Saint Petersburg, Russia, Vol. 1, pp. 244-250, International Association of Hydraulic Engineering and Research, Madrid, Spain,

Mercer, A.G., and Cooper, R.H. 1977. River bed scour related to the growth of a major ice jam. Proceedings, 3rd Canadian Hydrotechnical Conference, Quebec, Canadian Society for Civil Engineering, Montreal, Quebec, pp. 291-308.

Parkinson, F.E., and Holder, G.K. 1988. Ice jam development, release and surge wave propagation, Mackenzie River at Norman Wells. Proceedings of the Fifth Workshop on the Hydraulics of River Ice/ Ice Jams, June 21-24, 1988, Winnipeg, Manitoba, Subcommittee on Hydraulics of Ice-Covered Rivers, Associate Committee on Hydrology, National Research Council of Canada, Ottawa, Ontario, Canada, pp. 209-223.

Ponce, V.M., and Simons, D.B. 1977. Shallow wave propagation in open channel flow. Journal of the Hydraulics Division, ASCE, 103(HY12): 1461-1476.

Saadé, R. G., Sarraf, S., and El-Jabi, N. 1993. Numerical modelling of surges resulting from ice jam releases, Proceedings of the 11th Canadian Hydrotechnical Conference, Fredericton, N.B., June 8 to 11, 1993, Canadian Society for Civil Engineering, Montreal, Quebec, pp. 633-641.

Wong, J., Beltaos S., and Krishnappan, B.G. 1985. Laboratory tests on surges created by ice jam releases. Canadian Journal of Civil Engineering, 12 (4): 930-933.

Appendix A. Limits to leading-edge celerity, C_L

With reference to Eq. 1, it may be noted that, initially, both $\partial y/\partial t$ and $(S_f - S_o)$ are nil. The arrival of a wave causes them to take on non-zero, and most likely, positive values. This is self-evident in the case of $\partial y/\partial t$, but one cannot be certain about the sign of $(S_f - S_o)$. The latter can be expressed as

$$S_f - S_o = S_o\left(\frac{S_f}{S_o} - 1\right) = S_o\left[\left(\frac{U}{U_o}\right)^2\left(\frac{h}{h_o}\right)^{-4/3} - 1\right] \qquad [A.1]$$

which is based on the Manning resistance equation. In the vicinity of the leading edge, the rise in water level and the increase in flow depth are both very small relative to their respective unperturbed-flow values. Therefore, Eq. 2 reduces to:

$$\frac{U}{U_o} \approx 1 + \left(\frac{C_L}{aU_o} - 1 \right) \frac{\varepsilon}{h_o} \qquad [A.2]$$

in which $\varepsilon = h - h_o$, assumed to be much smaller than h_o for a very small rise in water level. Substituting Eq. A.2 in Eq. A.1 and neglecting terms involving powers of ε/h_o higher than one, it can be shown that

$$S_f - S_o \approx S_o \left[2\left(\frac{C_L}{aU_o} - 1 \right) - \frac{4}{3} \right] \frac{\varepsilon}{h_o} \qquad [A.3]$$

which will be positive for

$$C_L > \frac{5a}{3} U_o \qquad [A.4]$$

The RHS of Eq. A.4 can be identified as a generalized expression for the kinematic wave celerity. For a rectangular channel, a = 1, and thence Eq. A.4 gives $C_k = (5/3)U_o$. Had the Chezy resistance equation been used in place of the Manning equation, the numerical coefficient would have been 3/2 instead of 5/3. The measured waves that have been discussed in the preceding sections satisfy Eq. A.4. Therefore, a positive rate of rise at the early phase of wave arrival (when U and h are approximately equal to their unperturbed values) requires that

$$1 - a\frac{U_o^{\,2}}{gh_o} + \frac{C_L^{\,2}}{gh_o}\left(\frac{(1+a)U_o}{C_L} - 1 \right) > 0 \qquad [A.5]$$

which, after taking the positive root of the resulting quadratic, reduces to:

$$C_L < \frac{1+a}{2} U_o + \sqrt{gh_o + 0.25(1-a)^2 U_o^{\,2}} \qquad [A.6]$$

The RHS of Eq. A.6 can be identified as a generalized version of the gravity-wave celerity, which for a rectangular channel reduces to the more familiar expression $C_g = U_o + (gh_o)^{1/2}$. Under normal conditions, therefore, $C_k < C_L < C_g$. The same result is indicated by the linearized, small-amplitude theory (Ponce and Simons 1977) and by the nonlinear finite-amplitude theory of the monoclinal wave (Ferrick and Goodman 1998).

In the unlikely case that $(S_f - S_o)$ is negative at the start of the wave, a positive rate of rise can still occur, but the above conditions must be reversed, so that $C_k > C_L > C_g$. This requires that

$$\frac{U_o}{gh_o} \equiv F_o > \frac{3}{2a}\sqrt{\frac{2a}{5a-3}} \qquad [A.7]$$

in which F_o is the Froude number of the unperturbed flow. Because a is close (or equal) to 1, Eq. A.7 points to supercritical initial conditions (e.g. $F_o > 1.5$ for a rectangular channel). This is highly unlikely in ordinary rivers, and rendered even more improbable by the fact that jamming may not even be possible when the flow velocity is very high.